Optical nanofiber stretcher

Alexandre Matic,[1] Jacques Chrétien,[1] Adrien Godet,[1] Kien Phan HUY,[2] Jean-Charles Beugnot,[1,*]

[1] *Université de Franche-Comté, CNRS, institut FEMTO-ST, 25030 Besançon, France*
[2] *SUPMICROTECH-ENSMM, Université de Franche-Comté, CNRS, institut FEMTO-ST, 25030 Besançon, France*
[*] *jc.beugnot@femto-st.fr*

Abstract: Piezoelectric stretching of optical fiber is a technique that enables to create optical delays of few picoseconds, making it useful in a variety of applications in interferometry or optical cavities. Most commercial fiber stretchers involves few tens of meter lengths of fiber. Using a 120 mm long optical miro-nanofiber, we can create a compact optical delay line that achieves tunable delays of up to 19 picoseconds at telecommunications wavelengths. The high elasticity of silica and the micron scale diameter allow this significant optical delay to be achieved with low tensile force while keeping the overall length short. We successfully report both static and dynamic operation of this novel device. It could find application in interferometry and laser cavity stabilization, where short optical paths and strong resistance to environment would be required.

1. Main

Optical silica micro- and nanofibers have drawn much interest in the field of non-linear optics due to the strong confinement of light and large evanescent fields allowed by fiber dimensions close to the wavelength [1]. Many applications resulting from these exceptional properties have been investigated, such as optical fiber sensing [2], plasmonics [3], generation of light supercontinuum [4], nonlinear optics [5, 6], optomechanics [7, 8] or optical trapping [9, 10]. In addition to their remarkable optical properties, optical micro-nanofibers (ONF) also possess exceptional mechanical properties, particularly in terms of elasticity [11, 12]. Unlike commercially available 250 μm-diameter optical fibers that are limited to strains up to 0.2-0.3%, optical nanofibers can achieve a maximum strain of 4 to 6%. This exceptional mechanical property has enabled us to study the applications of optical delays for nanofibers and their use as a fiber stretcher. Fiber stretchers are notably used for producing optical delays for various applications such as interferometry [13], laser cavity stabilization [14] or fiber optic atmospheric optical turbulence sensors [15].

Most commercial fiber stretchers use classical 250 µm-diameter optical fiber and are limited by the stretching capacity of these fibers. For example, a 10 ps tunable delay requires a 2 m long standard SMF-28 optical fiber. Such long fibers increase sensitivity to thermal noise or vibrations and must be taken into account in the design of one's interferometer or laser cavity. Due to higher stretching capacity [16], optical nanofibers should allow reducing the length of the optical path of fiber tunable delay lines, reduce force requirement for stretching and improve stability due to shorter fiber length.

In this paper, we present a fiber stretcher using an ONF to produce an optical delay at telecommunication wavelength. The article is divided in three parts. In the first part, the theory behind our concept and the relationship between time delay, strain force and nanofiber diameter are presented. Then, we detailed the experimental characterization of the nanofiber stretcher and the measurement of the tunable delay. The last part is dedicated to dynamic operation.

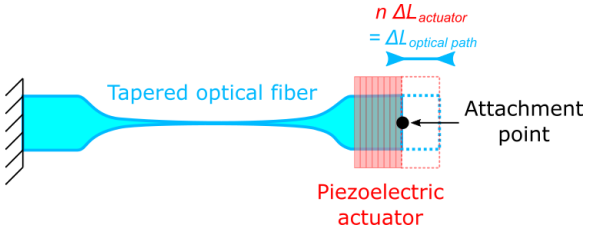

Fig. 1. Principle of a nanofiber stretcher using a tapered optical fiber and a piezoelectric actuator

In the following, we calculate the optical delay generated by a nanofiber stretched with given diameter and applied force, per millimetre of length. The distributed strain calculation show that 80% of the total elongation of the TOF is on the nanofiber [11]. We limit ourselves to the linear Hooke's law and consider only the tensile deformation of the nanofiber itself. The deformations due to the conical transitions between the standard optical fiber and the nanofiber are neglected.

The linear Hooke's law can be expressed as :

$$\frac{F}{S} = E \times \varepsilon = E \times \frac{\Delta L_{ONF}}{L_{ONF}}, \tag{1}$$

where F is defined as the applied force at the end of the nanofiber of section S, ε is the induced tensile strain on the silica nanofiber and $E = 73$ GPa is the silica Young's modulus. ΔL_{ONF} and L_{ONF} represent the stretch of the nanofiber subjected to the strain and the initial length of the nanofiber, respectively. Considering a nanofiber of diameter d with a section equal to $S = \pi.(d/2)^2$, Eq.(1) gives

$$F = E \times \frac{\Delta L_{ONF}}{L_{ONF}} \times \pi \left(\frac{d}{2}\right)^2. \tag{2}$$

The optical time delay Δt_{ONF} can be computed from the nanofiber stretch ΔL_{ONF} using

$$\Delta t_{ONF} = \Delta L_{ONF} \times \frac{n_{eff}(d)}{\mathrm{c}}, \tag{3}$$

where c is the speed of light in vacuum and $n_{eff}(d)$ is the effective refractive index of the optical mode propagating in the nanofiber for an ONF diameter d. We assume the taper is adiabatic so that only the fundamental mode of the ONF is present. The effective refractive index of the fundamental mode n_{eff} can be computed for any given diameter using analytic or numerical methods [17]. By combining Eq.(2) and (3), we obtain

$$\frac{\Delta t_{ONF}}{L_{ONF}} = \frac{2F n_{eff}(d)}{E\mathrm{c}\pi d^2}, \tag{4}$$

where we find on the left-hand side the optical delay per unit length and on the right-hand side a term proportional to the applied force. The results are shown in Fig. 2. The optical delay per unit of nanofiber length $\Delta t_{ONF}/L_{ONF}$ is plotted in false color as a function of the nanofiber diameter d and the applied force F. It can be seen that with a 1 μm diameter, for an applied force of 2.8 mN corresponding to a strain of 5%, an optical delay per unit of length of 0.2 ps/mm can be reached. Thus, a 120 mm long nanofiber should produce tunable delays of 20 ps with low applied force.

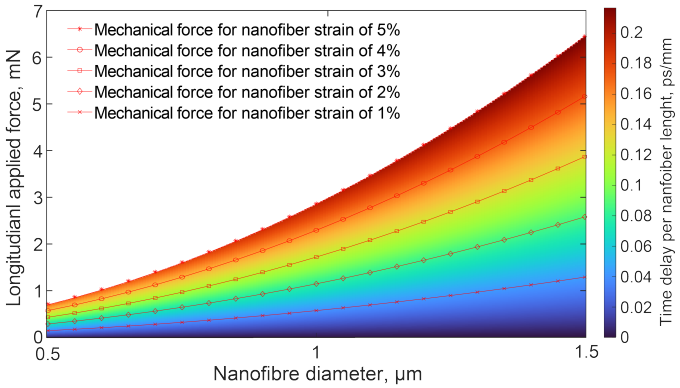

Fig. 2. 3D-map of applied strain force and corresponding time delay versus nanofiber diameter.

To validate these predictions, measurements were made on a 120 mm long ONF with a diameter of 1.0 $\pm$ 0.05 μm. Such a diameter allows single-mode propagation at λ =1550 nm avoiding multimodal interference. The total losses of the device including FC connectors are 1.38 dB and do not exceed 1.45 dB under repeated stretching. The fabrication losses are 0.2 dB and bending loss on packaging induce 1.1 dB. In order to measure the time delay induced by the deformation applied to the ONF, Optical Backscatter Reflectometry (OBR) was used with an OBR 4600. It allows localizing and characterize defects and events in our optical setup with a resolution of 10 µm using high-resolution Rayleigh scattering measurements. Fig. 3 shows a reflectometry profile

with the backscattered signal intensity as a function of the computed position. The ONF can be localized thanks to the increase of the back-scattered signal over few tens of millimetres.

Note that the OBR 4600 calculates the computed position from the measured optical delay using Eq. 3 and the effective refractive index of a SMF-28 optical fiber. The true position and length of the ONF can be calculated using the effective refractive index of the ONF fundamental mode $n_{eff} = 1.18$. In Fig. 3, the taper length which appears to be approximately 152 mm must then be corrected to $152 \times \frac{1.18}{1.5} \simeq 120$ mm.

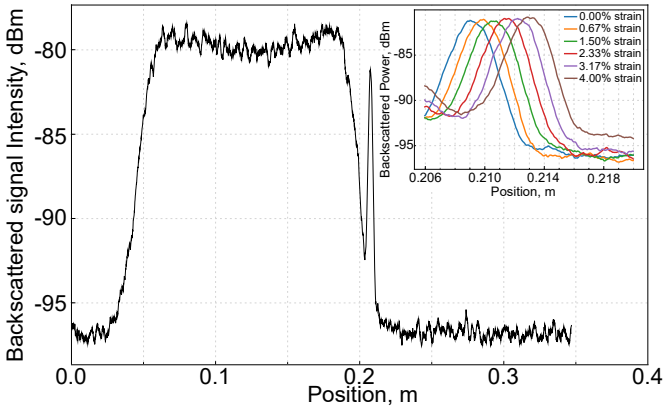

Fig. 3. Optical backscatter profile of an optical nanofiber. OBR profiles of the optical nanofiber zoomed on the defect zone, strained from 0 to 4%. Note that x-axis *computed position* is calculated by the OBR 4600 from the measured optical retardation of the Rayleigh scattered light.

In figure 3, we see a sharp peak around the position 0.2 m caused by a defect due to pollution or a manufacturing process problem. When the ONF is stretched, this peak shifts as shown in the inset at the top right of the figure 3. Thanks to the precise localization of this peak and the high resolution allowed by the OBR technique, we can measure both the effective stretch of the nanofiber and the induced time delay. Two Newport XML210 precision translation stages driven by the XPS Q8 controller are used to stretch the nanofiber from 0 to 4%. Taking into account the OBR and the translation stages resolutions, we can insure position with an 70 μm uncertainty.

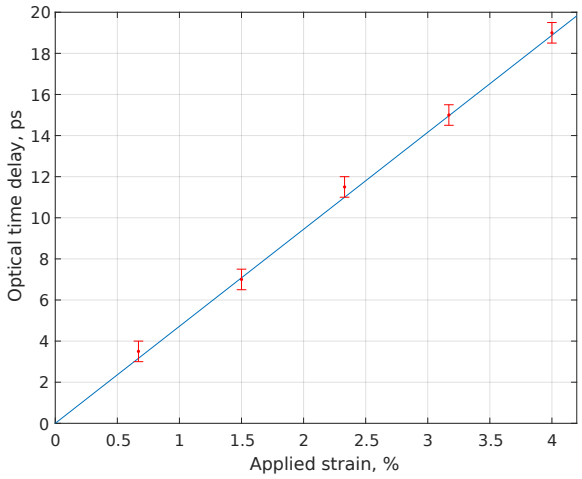

Fig. 4. Time delay versus applied strain, measurements (red points) and theory (blue line). The precision on the time delay measurement is 0.05 ps.

The applied strain is computed from the stages displacement similarly to, [16] while the optical time delay is deducted from the optical OBR measurements from Fig. 3. . The result are plotted with red dots in Fig. 4 showing a good linearity of the stretcher. Using Eq. 3 and the definition of the strain, $\varepsilon = \frac{\Delta L_{ONF}}{L_{ONF}}$ we can compute the delay

as a function of the strain

$$\Delta t_{ONF} = L_{ONF} \frac{n_{eff}(d)}{c} \varepsilon. \tag{5}$$

The results from equation 5 are shown in blue in Fig. 4, showing a very good agreement between theory and experiment. Considering that applied strain up to 6% have been reported for such nanofibers [16], time delay up to 28 ps could be reached. Higher delays can be achieved with longer nanofibers, but fabrication and packaging might become challenging for nanofiber lengths exceeding 140 mm. Eq. 5 shows that higher diameters could also improve time delay since the effective refractive index n_{eff} would increase, but single-mode condition limits the diameter above 1.07 µm at 1550 nm wavelength [18].

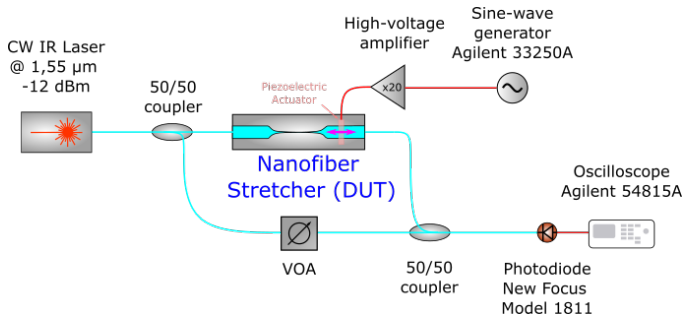

Fig. 5. Phase measurement setup based on a Mach-Zehnder interferometer. DUT: Device Under Test

Traditional fiber optic-based delay lines allow dynamic stretching up to few kHz while producing tens of picoseconds of delay thanks to piezoelectric actuators. Dynamic operation is required in many applications such as active stabilization of the length of an optical cavity or coherent optical tomography (OCT) for which it allows to scan one of the arms of the interferometer. To characterize our ONF fiber stretcher under dynamic operation, a piezoelectric actuator is used, as depicted in figure 1. One end of the fiber is fixed, while the second end is attached to the actuator. For this experiment, we have chosen to work with a Cedrat technologies APA40SM amplified piezoelectric actuator. These actuators consist of a traditional piezoelectric actuator surrounded by an elliptical metallic shell, which amplifies the deformation of the piezoelectric stack but reduces the resonance frequency of the system. This actuator is driven by a Cedrat Technologies LA75C high-voltage amplifier, allowing to amplify 20 times the voltage of a sine signal generated by an arbitrary waveform generator (Agilent 33250A). In order to measure the performance in terms of displacement in the harmonic regime, we use a Mach-Zehnder setup as shown in figure 5. The first arm contains the ONF stretcher, while the second arm contains a classical SMF-28 optical fiber and a variable optical attenuator (VOA) for arm-balancing. A continuous wave laser APEX AP3350A is used, with 1550 nm wavelength and output power at -12 dBm. At the end of the setup, light is collected by a New Focus 1811 IR photodiode and the electric signal is then analysed by an Agilent 54815A oscilloscope.

The oscilloscope acquires the voltage signal from the sine-wave generator used for actuation on the first channel, and the signal from the photodiode on a second channel. These signals are then retrieved and processed on a computer. An example of the signal is given in figure 6. The rise of the sine voltage is shown in blue, while the optical intensity is shown in red.

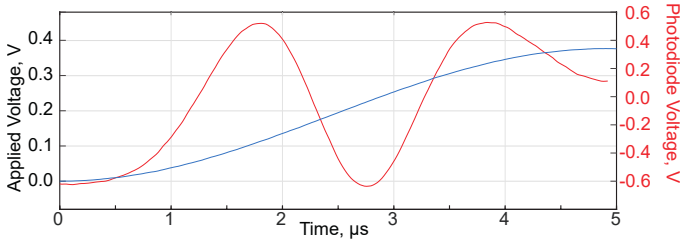

Fig. 6. Blue line: Voltage over time measured from sine generator output. Red line: photodiode output.

As the voltage rises (in blue), the optical nanofiber stretcher increases the length of the first arm of the Mach-Zehnder setup, and interferences are observed on the photodiode signal (in red). We can retrieve from the red curve the accumulated phase for a given voltage and deduce the optical path displacement. This is shown for two

frequencies 900 Hz and 10 kHz in Fig 7. We can see clearly hysteresis loops that can be explained by the piezoelectric actuator displacement hysteresis that is specified to be up to 10% by the manufacturer, which is consistent with our measurement. Note that this hysteresis is not a problem in applications in which the stretcher is used to stabilize the optical path and operated on a short dynamic range. Close-loop operation with the same actuator has been successfully reported in another mechanical system while still showing similar hysteresis behaviour [19]. For frequencies up to 12 kHz, we record the maximum voltage amplitude before harmonic distortion. We obtain a

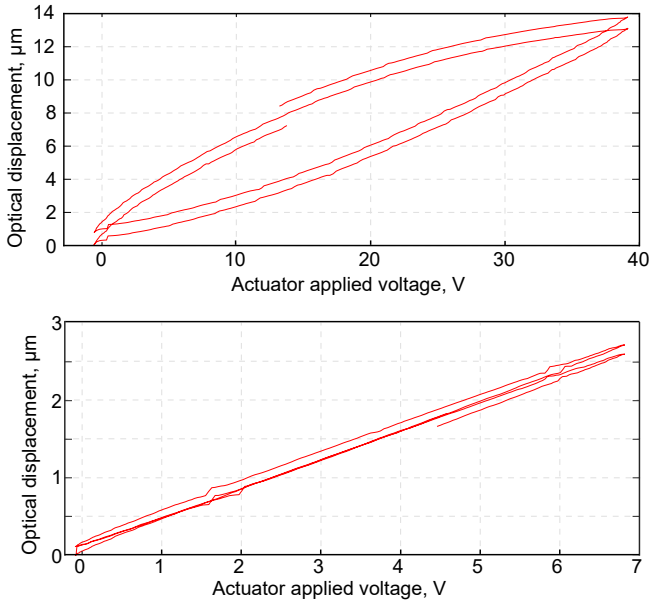

Fig. 7. Recorded optical displacement over voltage applied to the piezoelectric at 900 Hz (top) and 10 kHz (bottom).

corresponding maximum optical path displacement of more than 20 μm over a bandwidth of 900 Hz. Relative to the wavelength of the laser source, this represents a displacement of up to 13 λ, or about 10 fs in the time domain. Beyond this range, we measure the fundamental elastic mode of the piezoelectric actuator at $f_r = 1.7$ kHz and several elastic mode frequencies in the 10 kHz range. We also computed accumulated dispersion induced by the stretcher 0.05 ps/nm which is equivalent to 2.7 m of single mode fiber. Most commercial fiber stretcher would feature at least ten times this value. The results are summarized in table 1.

Results	
ONF length	120 mm
ONF diameter	1 μm
Total length (with connectors)	$\leq$ 50 cm
Optical path displacement	0.25 μm/V
Maximum optical displacement	20 μm
Max. optical displac. (at λ=1550 nm)	13 λ
Bandwidth	900 Hz
First resonance	1.7 kHz
Computed dispersion	500 ps/nm/km
Accumulated dispersion	0.05 ps/nm

Table 1. Dynamical parameter of nanofiber stretcher.

Compared to commercially available fiber stretchers, the values for dynamic operation might appear as low, as stretching lengths up to 3 mm from 1 to tens of kilohertz can be obtained for OCT applications where fast scanning and longer delays are required. In order to increase the scanning rate, a new mechanical design combined with a different actuator could help to increase the fundamental elastic mode frequency and thus the bandwidth. As far as the maximum achievable tunable delay, most commercial fiber stretchers typically use a few tens of meters of optical fiber rolled around cylinder or disk-shaped piezoelectric actuators [14]. This enables longer tunable delay,

but at a high cost in terms of initial delay and stability. Those devices are inherently sensitive to temperature variation or mechanical stress requiring careful packaging. On the opposite, a 120 mm fiber taper is easy to package and stabilize, making it much more robust with respect to thermal noise or vibrations. The nanofiber stretchers provides stretching up to 10λ which is enough for precise phase adjustment for most interferometry or laser cavity stabilization applications without increasing significantly the size of the interferometer or cavity. We believe this feature could be useful in novel applications for which the size of the interferometer or laser cavity has to remain small and stable. Finally, we measured a normalized optical path displacement of 0.25 μm/V which represents 0.25 % strain per volt. Typical commercial fiber stretcher 9×10^{-6} % strain per volt, showing the increased sensitivity to voltage thanks to lower force requirement.

In conclusion, we have demonstrated an optical nanofiber stretcher with a total length of less than 50 cm and a tunable delay range of unprecedented magnitude. We measured delay up to 19 ps at 1550 nm by using a 120 mm long tapered optical fiber with a diameter of 1 μm. The overall length of the ONF stretcher is two order of magnitude smaller than the length of a conventional optical fiber stretcher. With the ONF, the ratio of tunable optical delay to total length of the stretched fiber is better than that of a standard stretched fiber, while allowing the use of low-power, medium-voltage piezoelectric actuators [20]. We also have demonstrated dynamic linear operation below 900 Hz, which could be improved with a new mechanical design. We thus have proposed a compact, robust and low power solution for interferometer and laser cavity stabilization applications where short optical paths are required.

Funding. The authors acknowledge the financial support of EIPHI Graduate School (ANR-17-EURE-0002), and SATT Sayens.

Disclosures. The authors declare no conflicts of interest.

Data available. Data underlying the results presented in this paper are not publicly available at this time, but may be obtained from the authors upon reasonable request

References

1. G. Brambilla, "Optical fibre nanowires and microwires: A review," J. Opt. A: Pure Appl. Opt. 12, 043001 (2010).
2. P. Zhao, H. L. Ho, S. Fan, and W. Jin, "Evanescent wave lab-on-fiber for high sensitivity gas spectroscopy with wide dynamic range and long-term stability," Laser & Photonics Rev. p. 2200972 (2023).
3. R. K. Verma, A. K. Sharma, and B. D. Gupta, "Surface plasmon resonance based tapered fiber optic sensor with different taper profiles," Opt. Commun. 281, 1486–1491 (2008).
4. T. A. Birks, W. J. Wadsworth, and P. S. J. Russell, "Supercontinuum generation in tapered fibers," Opt. Lett. Vol. 25, Issue 19, pp. 1415-1417 25, 1415–1417 (2000).
5. M. A. Foster, A. C. Turner, M. Lipson, and A. L. Gaeta, "Nonlinear optics in photonic nanowires," Opt. Express, Vol. 16, Issue 2, pp. 1300-1320 16, 1300–1320 (2008).
6. J. C. Beugnot, S. Lebrun, G. Pauliat, H. Maillotte, V. Laude, and T. Sylvestre, "Brillouin light scattering from surface-acoustic waves in a subwavelength-diameter optical fibre," Nat. Commun. 2014 5:1 5, 1–6 (2014).
7. F. Tebbenjohanns, J. Jia, M. Antesberger, A. S. Prasad, S. Pucher, A. Rauschenbeutel, J. Volz, and P. Schneeweiß, "Feedback-cooling the fundamental torsional mechanical mode of a tapered optical fiber to 30 mk," arXiv preprint arXiv:2301.07792 (2023).
8. W. Xu, A. Iyer, L. Jin, S. Y. Set, and W. H. Renninger, "Strong optomechanical interactions with long-lived fundamental acoustic waves," Optica 10, 206–213 (2023).
9. K. S. Rajasree, T. Ray, K. Karlsson, J. L. Everett, and S. N. Chormaic, "Generation of cold rydberg atoms at submicron distances from an optical nanofiber," Phys. Rev. Res. 2, 012038 (2020).
10. S. Kato and T. Aoki, "Strong coupling between a trapped single atom and an all-fiber cavity," Phys. Rev. Lett. 115, 093603 (2015).
11. S. Holleis, T. Hoinkes, C. Wuttke, P. Schneeweiss, and A. Rauschenbeutel, "Experimental stress-strain analysis of tapered silica optical fibers with nanofiber waist," Appl. Phys. Lett. 104, 163109 (2014).
12. A. Godet, A. Ndao, T. Sylvestre, V. Pecheur, S. Lebrun, G. Pauliat, J.-C. Beugnot, and K. Phan Huy, "Brillouin spectroscopy of optical microfibers and nanofibers," Optica 4, 1232 (2017).
13. L. Delage and F. Reynaud, "Kilometric optical fiber interferometer," Opt. Express 9, 267 (2001).
14. D. A. Henderson, C. Hoffman, R. Culhane, and D. Viggiano III, "Kilohertz scanning all-fiber optical delay line using piezoelectric actuation," Fiber Opt. Sens. Technol. Appl. III, SPIE 5589, 99 (2004).
15. H. Mei, B. Li, H. Huang, and R. Rao, "Piezoelectric optical fiber stretcher for application in an atmospheric optical turbulence sensor," Appl. Opt. 46, 4371–4375 (2007).
16. A. Godet, T. Sylvestre, V. Pêcheur, J. Chrétien, J. C. Beugnot, and K. Phan Huy, "Nonlinear elasticity of silica nanofiber," APL Photonics 4, 080804 (2019).

17. L. Tong, R. R. Gattass, J. B. Ashcom, S. He, J. Lou, M. Shen, I. Maxwell, and E. Mazur, "Subwavelength-diameter silica wires for low-loss optical wave guiding," Nature 426, 816–819 (2003).
18. L. Tong, J. Lou, and E. Mazur, "Single-mode guiding properties of subwavelength-diameter silica and silicon wire waveguides," Opt. Express 12, 1025 (2004).
19. J. Correa and P. Ferreira, "Analysis and design for rapid prototyping mechanism using hybrid flexural pivots," Procedia Manuf. 1, 779 (2015).
20. J.-C. Beugnot, A. Godet, and J. Chretien, "Process for delaying an optical signal, ep2020/07854," (2020).